

**Wave Reflection and Transmission in Thin Beams in the
Presence of an Undamped Absorber**

H.M. El-Khatib, B.R. Mace and M.J. Brennan

ISVR Technical Memorandum 903

February 2003



SCIENTIFIC PUBLICATIONS BY THE ISVR

Technical Reports are published to promote timely dissemination of research results by ISVR personnel. This medium permits more detailed presentation than is usually acceptable for scientific journals. Responsibility for both the content and any opinions expressed rests entirely with the author(s).

Technical Memoranda are produced to enable the early or preliminary release of information by ISVR personnel where such release is deemed to be appropriate. Information contained in these memoranda may be incomplete, or form part of a continuing programme; this should be borne in mind when using or quoting from these documents.

Contract Reports are produced to record the results of scientific work carried out for sponsors, under contract. The ISVR treats these reports as confidential to sponsors and does not make them available for general circulation. Individual sponsors may, however, authorize subsequent release of the material.

COPYRIGHT NOTICE

(c) ISVR University of Southampton All rights reserved.

ISVR authorises you to view and download the Materials at this Web site ("Site") only for your personal, non-commercial use. This authorization is not a transfer of title in the Materials and copies of the Materials and is subject to the following restrictions: 1) you must retain, on all copies of the Materials downloaded, all copyright and other proprietary notices contained in the Materials; 2) you may not modify the Materials in any way or reproduce or publicly display, perform, or distribute or otherwise use them for any public or commercial purpose; and 3) you must not transfer the Materials to any other person unless you give them notice of, and they agree to accept, the obligations arising under these terms and conditions of use. You agree to abide by all additional restrictions displayed on the Site as it may be updated from time to time. This Site, including all Materials, is protected by worldwide copyright laws and treaty provisions. You agree to comply with all copyright laws worldwide in your use of this Site and to prevent any unauthorised copying of the Materials.

UNIVERSITY OF SOUTHAMPTON
INSTITUTE OF SOUND AND VIBRATION RESEARCH
DYNAMICS GROUP

**Wave Reflection and Transmission in
Thin Beams in the Presence of an
Undamped Absorber**

by

H.M. El-Khatib, B.R. Mace and M.J. Brennan

ISVR Technical Memorandum No: 903

February 2003

Authorised for issue by
Professor M.J. Brennan
Group Chairman

ABSTRACT

A wave propagates unchanged along a uniform member and if it is incident on a discontinuity, then part of it is reflected and the other part is transmitted (unless energy absorption exists in the discontinuity) with change in amplitude and/or phase.

The amplitudes of these reflected and transmitted waves are less than the amplitude of the incident wave. However, the amount of energy reflected and transmitted depends of the characteristics of the discontinuity.

The transmitted flexural waves may cause unpleasant consequences and serious damage to sensitive recipients through beam structures.

Complete suppression of those transmitted waves can be achieved at any frequency of interest by attaching a single tunable device.

Suppression of such waves has been achieved in the past by other workers over small range of frequencies. Improvements can be made to those tunable devices to obtain a satisfactory degree of suppression over a wide range of frequencies.

Simplicity of design and installation are of the main interests in the developed model.

This memorandum contains some background about tunable neutralisers, and an application of an undamped neutraliser to suppress the transmission of flexural waves on an Euler-Bernoulli beam with new independent tuning parameters.

TABLE OF CONTENTS

ABSTRACT.	i
TABLE OF CONTENTS	ii
LIST OF FIGURES	iv
GLOSSARY OF TERMS	v
 1- INTRODUCTION.	 1
 2- FLEXURAL WAVE MOTION IN BEAMS.	 2
2.1 Structural Wave Motion.	2
2.1.1 <i>Axial wave motion.</i>	2
2.1.2 <i>Torsional wave motion.</i>	3
2.1.3 <i>Flexural wave motion.</i>	4
2.2 Bending Waves in Beam Structures.	6
2.2.1 <i>Wave excitation in thin beams.</i>	6
2.2.2 <i>Flexural wave speed.</i>	8
2.2.3 <i>Effect of nearfield waves.</i>	9
2.3 Vibrational Power Transmission in Beams.	10
2.3.1 <i>Transmission of energy in farfield waves.</i>	10
2.3.2 <i>Energy flow in evanescent waves.</i>	12
2.3.3 <i>Energy flow in beams structures.</i>	13
2.4 Reflection and Transmission of Flexural Waves.	13
2.4.1 <i>Reflection & transmission coefficients.</i>	13
2.4.2 <i>Power reflection & transmission coefficients.</i>	15
 3- TUNING AN UNDAMPED VIBRATION NEUTRALISER ATTACHED TO A BEAM.	 17
3.1 Control of Flexural Waves of a Thin Beam.	17
3.2 Reflection & Transmission Coefficients.	19
3.3 Tuning the Neutraliser.	22
3.4 General Discussion.	23

4- NUMERICAL EXAMPLES.	24
4.1 Relation Between r , t , Ω and γ .	24
4.2 Conservation of Energy.	26
4.3 The Width Variation of the Transmission Stop – Band.	28
 5- CONCLUSION & DISCUSSION.	 31
5.1 General Concluding Remarks.	31
5.2 Future Work.	31
 APPENDICES.	 32
A1.0 r & t of flexural waves due to boundaries/discontinuities in beam structure.	32
A2.0 r & t of longitudinal waves due to boundaries/discontinuities in bar structures.	39
A3.0 Energy flow in the longitudinal travelling waves.	43
A4.0 Effect of undamped spring discontinuity on flexural waves.	44
A5.0 Using dynamic stiffness method in finding r & t of an undamped absorber.	45
A6.0 Relation between λ and Ω .	46
A7.0 Effect of mass discontinuity on flexural waves.	46
 REFERENCES.	 47

LIST OF FIGURES

- Figure 2.1 Rod element in axial vibration.
- Figure 2.2 Torsional motion of beam – like structure.
- Figure 2.3 Beam element vibrating in flexure.
- Figure 2.4 Definition of positive shear force and bending moment.
- Figure 2.5 Different propagating waves due to location of source of vibration. (a) Exciter is located on the x-axis at right angle to the z-axis. (b) exciter located at distance L from x-axis with slope to the z-axis. (c) Exciter pointing in the x-axis with a slope.
- Figure 2.6 Wave speed for acoustic & structural waves.
- Figure 2.7 Both kinds of waves around point impedance.
- Figure 3.1 An infinite thin beam with an undamped dynamic absorber.
- Figure 3.2 Shear forces and bending moments at either side of the absorber.
- Figure 3.3 Free body diagram of the absorber mass.
- Figure 4.1 Magnitude of the reflection and transmission coefficients as function of the frequency ratio Ω . (a) Reflection $|r|$; (b) Transmission $|t|$.
 — $\gamma=0.14$; $\gamma=0.1675$; ----- $\gamma=0.1975$; $\gamma=0.2250$;
 - - $\gamma=0.2525$; $\gamma=0.2825$;
- Figure 4.2 Power reflected and transmitted versus the frequency ratio Ω . (a) Reflection $|r|$; (b) Transmission $|t|$.
 — $\gamma=0.14$; $\gamma=0.1675$; ----- $\gamma=0.1975$; $\gamma=0.2250$;
 - - $\gamma=0.2525$; $\gamma=0.2825$;
- Figure 4.3 Conservation of energy for any given mass ratio.
- Figure 4.4 The effect of varying γ on Ω_i , Ω_r , and $\Delta\Omega$.
 — Ω_i ; Ω_r ; ----- $\Delta\Omega$.
- Figure A1.0 Flexural waves around the point discontinuity.
- Figure A4.0 Figure A4.0. Effect of Spring Discontinuity on the flexural waves in beam structures.
 (a) ———— $|t|$; ----- $|r|$.
- Figure A5.0 Figure A5.0. Free body diagram of the undamped absorber.
- Figure A7.0 Figure A7.0. Effect of mass discontinuity of flexural waves.

GLOSSARY OF TERMS

A	Cross sectional area.
a^+	Positive – going propagating wave.
a_N^+	Positive – going evanescent wave.
a^-	Negative – going propagating wave.
a_N^-	Negative – going evanescent wave.
b^+	Positive – going transmitting wave.
b_N^+	Positive – going transmitting evanescent wave.
c_B	Phase velocity.
c_g	Group velocity.
c_t	Damping constant.
e	Base of natural logarithm.
E	Young's modulus.
f	Frequency.
G	Shear modulus.
i	$\sqrt{-1}$.
I	Second moment of area.
k_f	Bending wavenumber.
k_l	Longitudinal wavenumber.
k_θ	Torsional wavenumber.
\bar{k}_t	Translational stiffness.
\bar{k}_R	Rotational stiffness
L	Length of beam.
m	Mass element.
m_d	Mass of the neutraliser.
M	Bending moment.
Q	Shear force.

r	Reflection coefficient.
R	Radius of curvature.
t	Transmission coefficient.
u	Displacement.
v	Velocity.
v^+	Velocity of positive propagating wave.
v_N^+	Velocity of positive evanescent wave.
w	Transverse displacement.
x	Longitudinal displacement.
y	Displacement of absorber mass.
\bar{Z}	Point impedance.
Z	Neutraliser impedance/beam impedance.
α	Neutraliser mass/beam mass.
α_r	Power reflection coefficient.
α_t	Power transmission coefficient.
β_i	Power flowing in incident wave.
β_r	Power flowing in reflected wave.
β_t	Power flowing in transmitted wave.
γ	Neutraliser mass/beam mass at neutraliser frequency.
Δ	Spacing between two accelerometers.
η	Structural damping loss factor.
θ	Torsional displacement.
λ	Wavelength.
ρ	Density.
ϕ	Phase velocity.
ω	Circular frequency.
Ω	Frequency ratio.
Ω_t	Tuned frequency.
Ω_l	Lower half – power point.

1- INTRODUCTION.

A vibration neutraliser wave model was developed in this report under idealised conditions. The optimal characteristics of a neutraliser modelled as point translational impedance of a thin beam were determined for optimal isolation.

The performance indicators such as the bandwidth under non – idealised conditions were determined.

The subject of adaptive – passive control has been the interest of many workers, for example reference [1-3].

Controlling the transmission of flexural waves on a Euler – Bernoulli beam has been investigated by Clark [4] and expanded by Brennan [5] to include optimally tuning parameters to suppress an incident propagating wave. The control used is a two – tier control system consisting of an open – loop part that tunes the neutraliser so that its natural frequency coincides with the forcing frequency, and a closed – loop control algorithm that fine tunes the neutraliser to suppress the incident propagating wave.

This report includes further investigation about the tuning parameters. The energy flowing in the thin beam due to propagation of waves and the intersection of opposite decaying nearfields has been modelled numerically.

The report consists of four chapters. An introduction about flexural wave motion in beams is introduced in Chapter 2.

Chapter 3, “Tuning an undamped vibration neutraliser attached to a beam,” presents an introduction about tunable neutralisers and the proposed tuning parameters to suppress the incident propagating waves using an undamped neutraliser. Reflection and transmission of the different flexural waves were also been included.

Chapter 4, “Numerical Examples,” present the results concerning the numerical simulations performed. The first law of thermodynamics “Energy Conservation” has been satisfied. The width variation of the transmission stop – band is included.

The most important remarks obtained from the numerical work are introduced in Chapter 5 “Conclusions & Discussion”. In addition to the scheduled future work in this area.

2- FLEXURAL WAVE MOTION IN BEAMS.

The elastic wave motion in one – dimensional structures is addressed in this chapter specifically beam structures. The three principle types of structural wave motion (axial, torsional, and flexural) through which energy may propagate through the structure are introduced in the first section. The second section highlights the bending waves in beam like structures. Expressions of vibrational power flow were derived in the third section, from knowledge of flexural wave motion in beam structures. Finally, reflection and transmission of flexural waves due to boundary conditions and discontinuities were briefly described.

2.1 Structural Wave Motion.

Waves are everywhere in nature. A wave can be described as a disturbance that travels through the medium from one location to another. To fully understand the nature of a wave, it is important to consider the medium as a series of interconnected elements or particles. The interaction of one element in the medium with the next adjacent one allows the disturbance to travel through the medium. Waves come in many shapes and forms. While all waves share some basic characteristic properties and behaviours.

The three principle types of structural wave motion are introduced in this section.

2.1.1 Axial wave motion.

Figure 2.1, below shows an element of a rod, δx , undergoing longitudinal motion. The wave in which the direction of the disturbed particles coincides with the direction of wave propagation is defined as longitudinal wave. It should be noted that pure longitudinal motion could only occur in solids whose dimensions are much greater than the resulting wavelength.

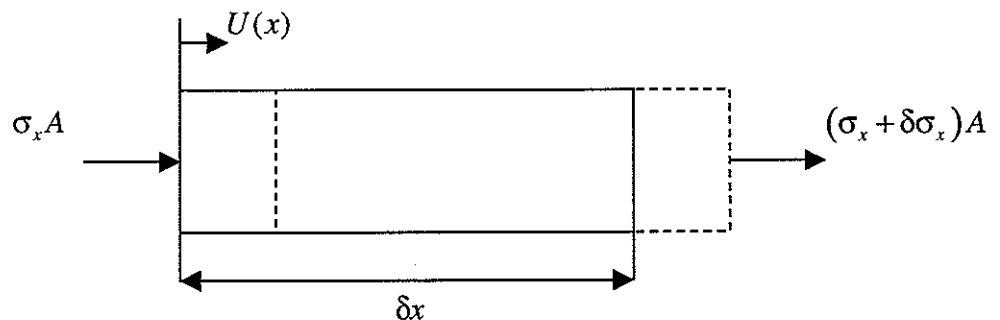


Figure 2.1. Rod element in axial vibration.

Consideration of the dynamic equilibrium of the element, δx , in terms of the applied torque, δT , and the resulting angular acceleration, $\partial^2\theta/\partial t^2$, gives the pure torsional wave equation for a circular section bar.

$$G \frac{\partial^2 \theta}{\partial x^2} = \rho \frac{\partial^2 \theta}{\partial t^2}, \quad (2.3)$$

where G and θ represents the shear modulus and the angular displacement respectively. The required solution to Eq.(1.3) may be given by

$$\theta(x) = a^+ e^{-ik_\theta x} + a^- e^{ik_\theta x}, \quad (2.4)$$

where $k_\theta = \omega\sqrt{\rho/G}$ is the torsional wavenumber.

2.1.3 Flexural wave motion.

When a beam is excited transversely, it gives rise to flexural wave motion in the structure. If the frequency of excitation is low, i.e. the resulting wavelength is large compared to the beam dimensions then the high frequency effects associated with the shear deformation and rotary inertia of the cross section can be assumed to be negligible. The inclusion of these terms for high frequency beam vibration is termed "Timoshenko" beam theory [9]. If however, those additional terms can be ignored then simpler "Euler-Bernoulli" expressions can be used to describe the beam motion. Figure 2.3, shows an element of a beam, δx , vibrating in flexure. Inherent in the assumptions relating to Euler-Bernoulli beam, theory is approximation that plane sections remain plane and perpendicular to the neutral axis of bending.

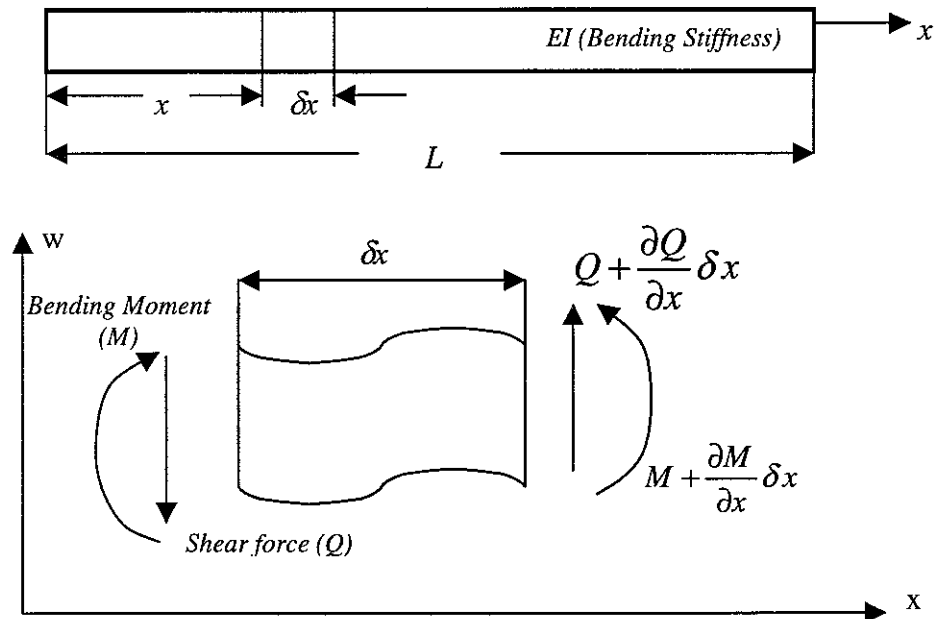


Figure 2.3. Beam element vibrating in flexure.

The sign convention adopted is shown in Figure 2.4 together with the forces and moments acting on an elemental length of the beam in its distorted form.

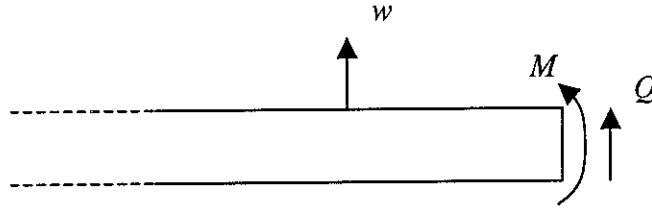


Figure 2.4. Definition of positive shear force and bending moment.

The corresponding shear force Q and bending moment M as defined in Figure 2.4 are then

$$Q = -EI \frac{\partial^3 w}{\partial x^3}, \quad M = EI \frac{\partial^2 w}{\partial x^2}.$$

Consideration of the dynamic equilibrium of the beam element results in the Euler-Bernoulli flexural wave equation as derived in [10].

$$EI \frac{\partial^4 w}{\partial x^4} + \rho A \frac{\partial^2 w}{\partial t^2} = 0. \quad (2.5)$$

For simple harmonic motion $w(x, t) = W(x)e^{i\omega t}$, the equation of motion becomes

$$EI \frac{d^4 W}{dx^4} - \rho A \omega^2 W = 0. \quad (2.6)$$

Again the solution to this fourth order equation is given in many well-established texts on mechanical vibrations as follows:

$$w(x) = a^+ e^{-ik_f x} + a^- e^{ik_f x} + a_N^+ e^{-k_f x} + a_N^- e^{k_f x}, \quad (2.7)$$

where

$$k_f = \sqrt[4]{\rho A / EI} \sqrt{\omega}, \quad (2.8)$$

is the flexural wavenumber and ω is the circular frequency while ρ , A , and EI have their usual meanings. Hereafter k will hold the meaning of flexural wavenumber.

The displacement of the beam structural element is considered as the sum of the four wave components. Two farfield propagating waves; the positive – going a^+ and the negative – going a^- wave. In addition to these propagating waves, a set of nearfield or non – propagating evanescent waves, a_N^+ in the positive direction and a_N^- in the negative direction. These evanescent waves are only of significant interest in the

nearfield of a source or discontinuity. Their amplitudes decrease rapidly with distance by a factor of over 500 in one wavelength [11], and can therefore be ignored at sufficiently large distances.

From Figure 2.3, flexural waves cause two internal loads to act on a beam element, a shear force (Q) and a bending moment (M).

Considerations of both these loads is important, where these may help in analysing wave motion and components of power transmission.

However, there is another importance of taking evanescent waves under consideration in the nearfield of a sound where the intersection of two evanescent waves of opposite directions may produce some energy as will be shown later.

2.2 Bending Waves in Beam Structures.

Bending or flexural waves are by far the most important for sound radiation because of the rather large lateral deflections associated with them. These waves are easy to excite in beam structures and cause serious effects.

Since this work is primarily concerned with the vibrations of beam – like structures representative of an infinite thin beam, the following will be related to flexural wave motion.

This section introduces the possible excitations in thin beams, the characteristics of flexural waves, and a brief description of the evanescent waves.

2.2.1 Wave excitation in thin beams.

There are two other major types of waves may propagate through beam structures besides the bending waves. Although the flexural waves are the most dominant due to simplicity in excitation.

Figure 2.5 shows the possible propagating waves due to location of the excitation point.

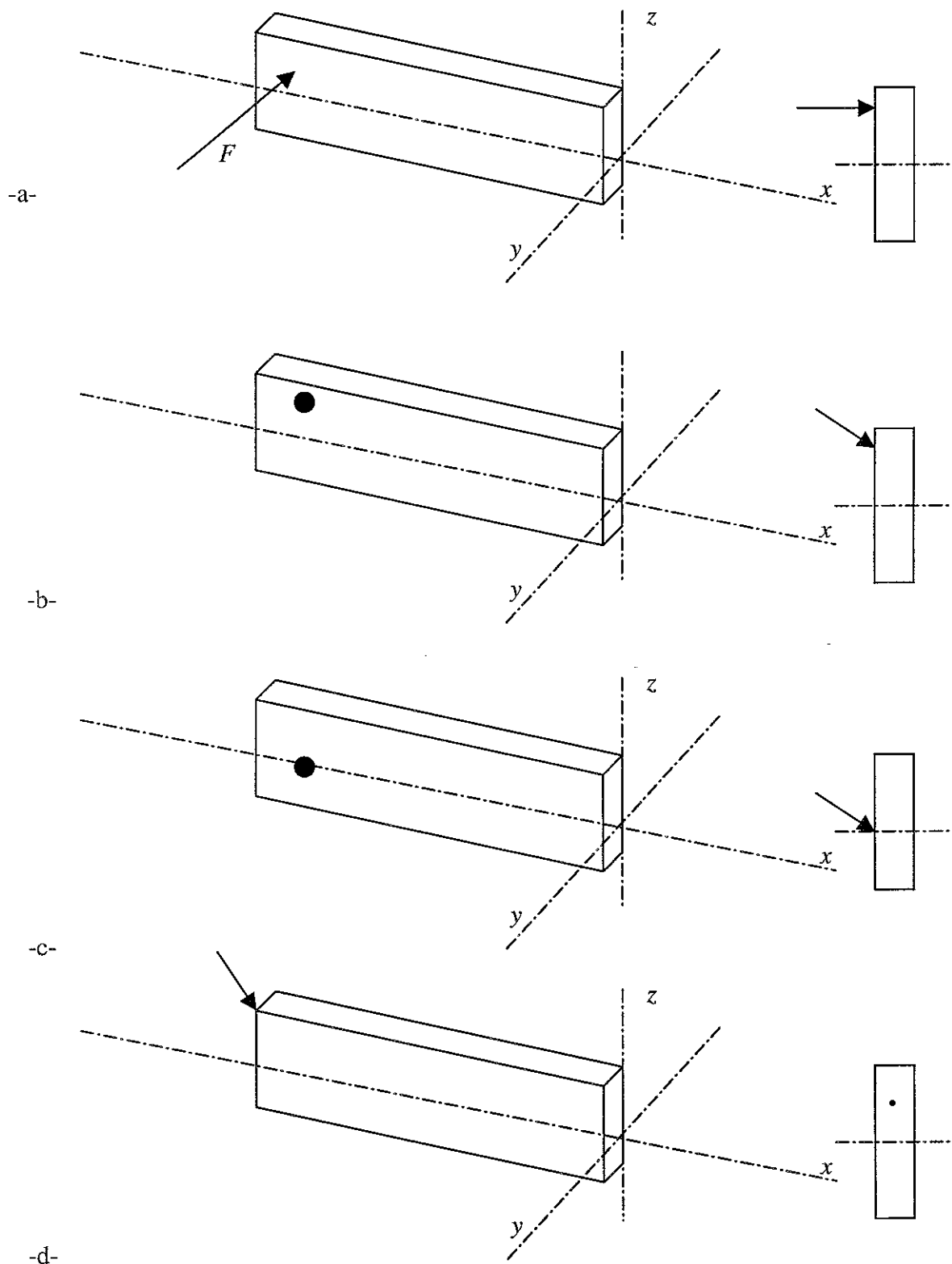


Figure 2.5. Different propagating waves due to location of source of vibration.

- (a) Exciter is located on the x-axis at right angle to the z-axis.
- (b) Exciter is located at distance L from x-axis with slope to the z-axis.
- (c) Exciter pointing at x-axis with slope to z-axis.
- (d) Exciter pointing in the direction of x-axis with a slope.

Flexural vibrations in the y-axis and torsional vibrations about the x-axis are excited in the model given in Figure 2.5(a) as well as the one in Figure 2.5(b) besides exciting the flexural vibration in the stiff direction (z-axis).

The model given in Figure 2.5(c) may include flexural vibration in both y and z directions. While the model in Figure 2.5(d) may include longitudinal waves in the x-direction (difficult to excite), flexural waves in z-axis.

When two or more constituent travelling waves of same amplitude $A_1 = A_2$ adds up, they may give a standing wave, which includes significant nodes (points with no displacement) and antinodes (points with large displacement), e.g. if $A_1 = A_2$ is real this is

$$y(x, t) = A_1 \cos(\omega t + kx) + A_1 \cos(\omega t - kx), \quad (2.9)$$

hence,

$$y(x, t) = 2A_1 \cos(\omega t) \cos(kx). \quad (2.10)$$

It is also possible to construct a travelling wave out of two standing waves, $\pi/2$ out of phase in time and space.

$$y(x, t) = A_1 \cos(\omega t) \cos(kx) + A_1 \sin(\omega t) \sin(kx) = A_1 \cos(\omega t - kx). \quad (2.11)$$

Flexural waves are unlike other wave types, must be represented by few field variables instead of two, and the boundary conditions are more complex.

2.2.2 Flexural wave speed.

The speed at which a disturbance (wave) propagate in a structure is defined as the phase velocity (c_B) and it is given by

$$c_B = \omega / k = \sqrt[4]{EI / \rho A} \cdot \sqrt{\omega}, \quad (2.12)$$

Therefore c_B is a frequency dependent as show in Figure 2.6. Hence flexural waves are dispersive and radiate sound strongly beyond the coincidence frequency f_c^* .

Note that the speed at which energy propagate through structures is called group velocity $c_g = \partial \omega / \partial k$. One can find from Eq.(2.12) that the group velocity is twice the phase velocity for flexural waves in a beam, On the other hand $c_B = c_g$ for non-dispersive systems.

* Coincidence frequency is the frequency at which the flexural waves will have the same speed as the sound in air $340ms^{-1}$

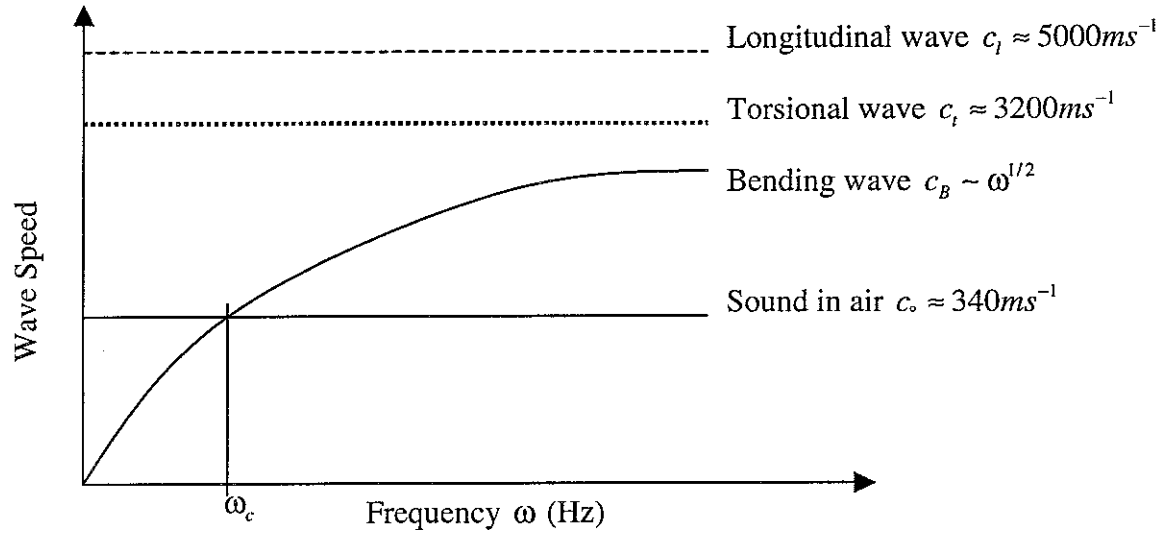


Figure 2.6. Wave speed for acoustic and structural waves.

It worth mentioning that beam structures retain two unique properties can be used in differencing bars and beams. These are

- Flexural waves are dispersive.
- The displacement of the beam element may consists of four wave components.

Thus flexural wave motion in beam structure can be approximated by a shear wave instead of longitudinal one in bars.

2.2.3 Effect of nearfield waves.

Inspecting the two nearfield components in Eq.(2.7) will appeal the (negative) real exponent shows that the motion is not harmonic with respect to position along the beam. In another words, for a given instant of time, the entire wave has the same sign. The motion is in phase for all x , and the negative exponential term shows the motion decays in the positive x -direction. Waves with these properties are called non – propagating (evanescent) waves.

These waves cannot be seen at large distances from where they are generated. Because of this they are also called nearfield waves.

2.3 Vibrational Power Transmission in Beams.

This section present an introduction to power flow analysis in beam structures. The effect of boundaries and discontinuities on power flow also included.

2.3.1 Transmission of energy in farfield waves.

Power is the rate at which work is done. As the wave travels down the beam, the beam has associated kinetic and potential (spring – like) energies as explained by Cremer [6]. To illustrate this consider a positive travelling flexural wave with real amplitude for energy calculation a^+ , therefore

$$w(x, t) = \text{Re} \left\{ a^+ e^{i(\omega t - kx)} \right\} = a^+ \cos(\omega t - kx). \quad (2.13)$$

consider a small element of length δx . thus the kinetic energy per unit length $1/2\rho A (\partial w / \partial t)^2$ is given by

$$E_{kin} = \frac{1}{2} \rho A \omega^2 a^{+2} \sin^2(\omega t - kx), \quad (2.14)$$

and the potential energy per unit length $1/2EI (\partial^2 w / \partial x^2)$ is given by

$$E_{pot} = \frac{1}{2} \rho A \omega^2 a^{+2} \cos^2(\omega t - kx), \quad (2.15)$$

Note that $EIk^4 = \rho A \omega^2$. therefore the total energy per unit length is

$$E_{tot} = E_{kin} + E_{pot} = \frac{1}{2} \rho A |v^+|^2, \quad (2.16)$$

where $v^+ = \omega a^+$ is the velocity amplitude. These were given in many textbooks as [6,10].

The corresponding shear force $Q = -EI \partial^3 w / \partial x^3$ and bending moment $M = EI \partial^2 w / \partial x^2$ as defined in Figure 2.4 transmit power.

The instantaneous intensity $i(x, t)$ is given in terms of the beam deformation and internal forces by Mace [12]

$$i(x, t) = -Qv - M\dot{\theta}, \quad v = \frac{\partial w}{\partial t}, \quad \dot{\theta} = \frac{\partial^2 w}{\partial x \partial t}, \quad (2.17)$$

where v and $\dot{\theta}$ are the transverse and rotational velocities of the beam. Therefore one can find the instantaneous intensity of the positive propagating wave from Eq.(2.16)

$$i(x, t) = \rho A \omega^2 c_B a^{+2} = c_g E_{tot}. \quad (2.18)$$

Therefore the energy per unit time is the product of the total energy per unit length (E_{tot}) and the group velocity (c_g).

The time – average intensity $\langle i(t) \rangle$ may be of most interest in many applications and it can be found by time – averaging the instantaneous intensity.

$$\langle i(t) \rangle = \frac{\omega}{2\pi} \int_0^{2\pi/\omega} I(t) dt \quad (2.19)$$

This was found to have a value equal to the instantaneous intensity. Where both Q and M exerts equal amount of work when averaged over a cycle.

The power flow can also be found using the characteristic impedance (Z)*of the wave [13] which can be defined as the ratio of the internal force to the resulting velocity at a given point of the structure when a wave propagate.

$$i(x, t) = \frac{1}{2} Z |v^+|^2, \quad (2.20)$$

where

$$Z = \frac{|EI \partial^3 w / \partial x^3|}{|\partial w / \partial t|} = \rho A c_B. \quad (2.21)$$

Thus the power flow for both propagating waves was found.

$$\frac{1}{2} \rho A \omega^2 c_g \left\{ |a^-|^2 + 2 |a^-| |a^+| \cos(2\omega t + \phi_1 + \phi_2) + |a^+|^2 \right\}, \quad (2.22)$$

Hence three terms are involved in the power flowing due to propagation of the two flexural waves a^+ and a^- . The power flowing due to both propagating waves and the cross-energy term, which is a frequency dependent. ϕ_1 and ϕ_2 are the phase shifts in the positive and negative propagating wave respectively (the wave amplitudes may be complex).

* Analysis of the input impedance of beams in flexure is somewhat more difficult because the propagating velocity is frequency dependent and also because of the existence of nearfields.

2.3.2 Energy flow in evanescent waves.

It is generally accepted that farfield waves can transmit energy and nearfield waves hold energy, but they cannot transmit it through the structure [14]. This has been proven numerically.

Consider an evanescent flexural wave, with real amplitude a_N^+ , therefore

$$w(x, t) = \text{Re}\{a_N^+ e^{(i\omega t - kx)}\} = a_N^+ e^{-kx} \cos(\omega t). \quad (2.23)$$

The total energy per unit length for the positive – going evanescent found below

$$E_{tot} = \frac{1}{2} \rho A |v_N^+|^2, \quad (2.24)$$

where $v_N^+ = \omega a_N^+$ is the velocity amplitude of the positive – going evanescent wave.

One can find that the total rate of work has a zero value using Eq.(2.16).

While the energy flow in a solitary evanescent wave is zero, two such waves of opposite directions can produce non – zero flow of energy.

This energy flow is the result of the interaction of the waves. It is the result of the spatial co-ordinate, and doesn't contradict the energy conservation law [9], and this has also been shown numerically.

Consider two evanescent waves decaying in opposite directions, therefore

$$w(x, t) = |a_N^+| e^{-kx} \cos(\omega t + \phi_1) + |a_N^-| e^{kx} \cos(\omega t + \phi_2) \quad (2.25)$$

One can find that the total energy flow through a beam cross-section thus consists of three terms.

$$i(x, t) = \rho A \omega^2 \left[|a_N^+|^2 e^{-2kx} + 2 |a_N^+| |a_N^-| \cos(\phi_1 - \phi_2) + |a_N^-|^2 e^{2kx} \right] \quad (2.26)$$

One of the three terms in Eq.(2.26) indicates that there is a cross – flow of energy between the two evanescent waves, which is independent of the spatial co-ordinate. When the displacements in the two opposite evanescent waves are not in phase, and not in counter-phase, the work done by the stresses in one wave through the displacements in the other wave is not zero, and that leads to a uniform flow of energy along the structure.

2.3.3 Energy flow in beam structures.

The total energy flowing in a beam cross-section was found below, considering the existence of the four wave components.

$$w(x, t) = |a_N^-| e^{kx} \cos(\omega t + \phi_1) + |a_N^+| e^{-kx} \cos(\omega t + \phi_2) + |a^-| \cos(\omega t + kx + \phi_3) + |a^+| \cos(\omega t - kx + \phi_4). \quad (2.27)$$

Therefore

$$i(x, t) = \frac{1}{2} \rho A \omega^2 c_B \left\{ \begin{aligned} & -|a_N^-| |a^-| e^{kx} (\sin(2\omega t + kx + \phi_1 + \phi_3) - \cos(2\omega t + kx + \phi_1 + \phi_3)) \\ & -|a_N^-| |a^+| e^{kx} (\sin(2\omega - kx + \phi_1 + \phi_4) + \cos(2\omega - kx + \phi_1 + \phi_4)) - |a^-|^2 \\ & +|a_N^+| |a^-| e^{-kx} (\sin(2\omega t + kx + \phi_2 + \phi_3) + \cos(2\omega t + kx + \phi_2 + \phi_3)) + |a^+|^2 \\ & +|a_N^+| |a^+| e^{-kx} (\sin(2\omega t - kx + \phi_2 + \phi_4) - \cos(2\omega t - kx + \phi_2 + \phi_4)) \\ & 2|a_N^-| |a_N^+| \sin(\phi_1 - \phi_2) \end{aligned} \right\} \quad (2.28)$$

The total energy flow through a beam cross-section consists of seven terms. two terms are readily recognised as the propagating pair (a^+ and a^-). The rest of the five terms represents the cross-flow of energy between the different flexural waves as shown in the equation above. They are dependent on both spatial and time co-ordinates except the cross-flow energy between the positive and negative evanescent waves.

2.4 Reflection & Transmission of Flexural Waves.

A wave propagates unchanged along a uniform member, if incident on a boundary or point discontinuity then its status will change [15].

This section introduces some basic knowledge about reflection and transmission of waves for famous boundary/discontinuity conditions. This will form a solid base in order to solve cases with complex discontinuities (undamped neutraliser) as will be seen in later chapters.

2.4.1 Reflection & transmission coefficients.

An incident wave (a^+ and/or a_N^+) upon a boundary gives rise to reflected wave (a^- and/or a_N^-). While a wave incident (a^+) upon a discontinuity gives rise to reflected (a^-, a_N^-) and transmitted waves (b^+, b_N^+) of both kinds (nearfield and

farfield waves) as shown in Figure 2.7. Whose amplitudes may be found from the well – known reflection and transmission coefficients [6], thus

$$\frac{a^-}{a^+} = r; \frac{a_N^-}{a^+} = r_N; t = \frac{b^+}{a^+}; t_N = \frac{b_N^+}{a^+}, \quad (2.29)$$

where r and t are the reflection and transmission coefficients respectively. The subscript N refers to reflection (r_N) or transmission (t_N) of the nearfield waves.

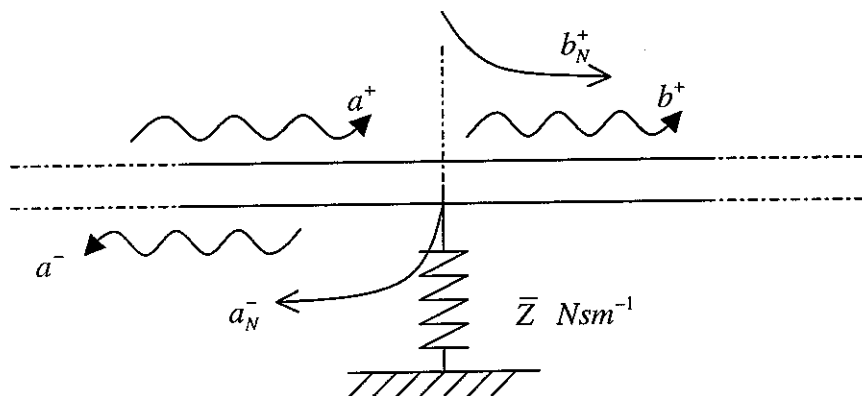


Figure 2.7. Both kinds of waves around point impedance.

Consider a propagating wave (a^+) incident upon point impedance (general case), it will give rise to far- and nearfield waves as shown in Figure 2.7.

The reflection and transmission coefficients can be found by considering the continuity and equilibrium equations of the system.

Continuity of displacement gives $w_+(0) = w_-(0)$ and hence

$$a^+ + a^- + a_N^+ = b^+ + b_N^+, \quad (2.30)$$

Continuity of rotation ($\partial w_+(0)/\partial x = \partial w_-(0)/\partial x$) gives

$$-ia^+ + ia^- + a_N^- = -ib^+ - b_N^+ \quad (2.31)$$

From the balance of the shear forces and bending moments at cross sections of the beam at either side of the point impedance Z , then one can derive the following relations.

$$-a^+ - a^- + a_N^- = -b^+ + b_N^+, \quad (2.32)$$

and from the force equilibrium

$$ia^+ - ia^- + a_N^- - ib^+ + b_N^+ = Z(b^+ + b_N^+), \quad (2.33)$$

where $Z = i\bar{Z}\omega / Elk^3$ is a dimensionless factor indicates the ratio of the spring point impedance to the beam impedance. Therefore r , t , and r_N ($r_N = t_N$) were found and these are

$$\begin{aligned} r &= \frac{iZ}{4 - Z(1+i)} \\ t &= \frac{4 - Z}{4 - Z(1+i)} \\ r_N &= \frac{Z}{4 - Z(1+i)} \end{aligned} \quad (2.34)$$

Replacing this point impedance with the impedance of either mass, damper, or spring, then the above equations are satisfied. Where equating \bar{Z} with either impedance of mass ($\bar{Z}_{mass} = i\omega m$), damper ($\bar{Z}_{damper} = \bar{c}_t$), or spring ($\bar{Z}_{spring} = \bar{k}_t / i\omega$), will result in the dimensionless factor Z of each of the three elements. This dimensionless factor Z has the same value obtained for each other element as shown in Appendix A1.0, which contains the reflection and transmission coefficients of many well-known models.

If the point impedance is assumed to be infinite, then it will be considered as pinned discontinuity where

$$r = -\frac{(1+i)}{2}; t = \frac{(1-i)}{2}; r_N = t_N = \frac{(i-1)}{2}. \quad (2.35)$$

2.4.2 Power reflection & transmission coefficients.

The farfield waves cause motion where they allow energy to flow through a structure while nearfield do not as explained previously.

The power flow is proportional to the square of the wave amplitude as found from Eq.(2.22) where the beam's mass per unit length doesn't change.

The power reflection α_r and transmission α_t coefficients play an important role in expressing the amount of power flowing and reflection through a discontinuity. These can be found below

$$\alpha_r = \frac{\beta_r}{\beta_i}; \quad \alpha_t = \frac{\beta_t}{\beta_i}, \quad (2.36)$$

where β_r , β_t , and β_i represents the reflected wave energy, transmitted wave energy, and the incident wave energy respectively.

The power reflection and transmission from the previous model shown in Figure 2.7 are found below

$$\alpha_r = \frac{1}{2} \frac{|a^-|^2}{|a^+|^2} = 0.5 = \alpha_t. \quad (2.37)$$

Those for the pin joint discontinuity α_r and $\alpha_t = 0.5$, therefore if there is no energy loss at the discontinuity (damping element) then

$$\alpha_r + \alpha_t = 1. \quad (2.38)$$

A thorough investigation of longitudinal waves propagating in bar structures was performed. Reflection r and t transmission coefficients of the propagating waves were found for various discontinuities and boundaries. These are attached in Appendix A2.0. In addition, the energy flow in the longitudinal travelling waves was found and attached in Appendix A3.0.

3- TUNING AN UNDAMPED VIBRATION

NEUTRALISER ATTACHED TO A BEAM.

This chapter describes the effects on the reflection and transmission of waves in an infinite Euler-Bernoulli beam by attaching an undamped passive vibration absorber. The chapter comprises four sections. The first section introduces a brief background while the second one derives the reflection and transmission coefficients of both farfield and nearfield waves due to attaching an undamped vibration absorber to the beam. The third section describes a simple relation between the tuning frequency and the mass ratio. The final section includes a general discussion.

3.1 Control of Flexural Waves of a Thin Beam.

The use of tunable neutralisers to control the flexural waves on an infinite Euler-Bernoulli beam have been the subject of many workers. More interest has been paid to the adaptive-passive control in the past few years. This offers simplicity in the design and a much lower cost than active control, for example references [1-3]. The stiffness of the absorber is changed until its tuned frequency coincides with the forcing frequency, hence the maximum impedance is applied at the frequency of interest. Previous work by Brennan [5] on tunable neutralisers presented an improved model of a tunable neutraliser. Expressions for the reflection and transmission coefficients of the propagating waves were derived as well as for the tuned frequency, in order to control the transmission of the propagating incident waves. Zero transmission at a single frequency was seen for an undamped neutraliser. The bandwidth according to Brennan [5] will be zero for an undamped absorber. However, the bandwidth was defined as the range of frequencies over which the modulus of the transmitted wave is within 3 dB of the minimum. It was found that the damping controls the bandwidth and it was shown that the bandwidth of the neutraliser with a small mass ratio is equal to the loss factor (η), and it equals $4\eta/3$ the loss factor for a large mass ratio. It was found that, in order to increase the bandwidth while maintaining the same attenuation of the flexural waves, then the mass of the neutraliser has to be increased proportionately.

This report introduces a new definition for the bandwidth of the undamped neutraliser, new independent tuning parameters, and reflection and transmission coefficients of both propagating and evanescent waves in terms of wave amplitudes which can be estimated experimentally using the wave decomposition approach.

It was demonstrated previously that a complete suppression of flexural waves could be achieved theoretically with an undamped spring fitted between a rigid foundation and a beam as given in Appendix A4.0. The amount of damping is inversely proportional to the wave suppression as investigated by Brennan [5].

Consider the effect of an undamped passive-dynamic absorber as shown in Figure (3.1) on the reflection and transmission of waves in a beam-like structure. Here m and \bar{k}_t represents the mass and stiffness of the absorber. If waves are incident on the discontinuity, then some of the waves will be transmitted and some will be reflected. The reflection and transmission coefficients depend on the characteristics of the passive absorber.

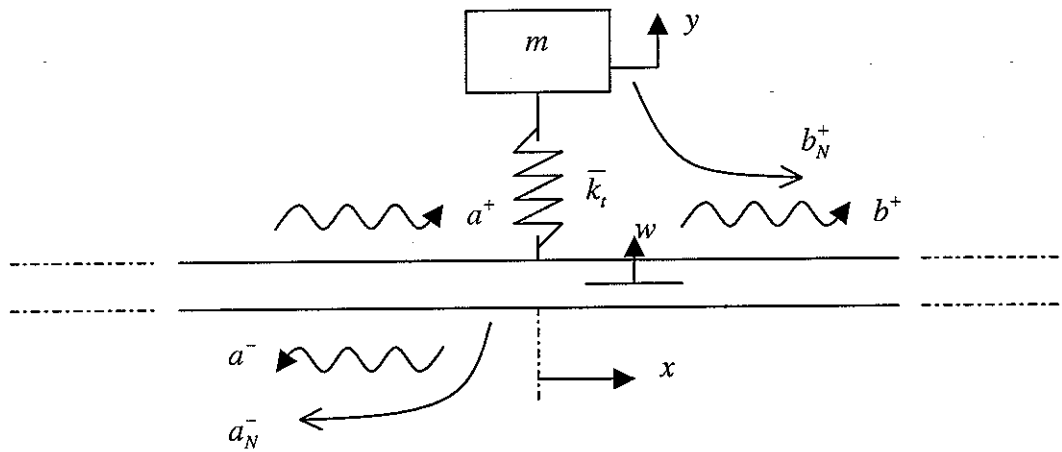


Figure 3.1 An infinite thin beam with an undamped dynamic absorber.

The beam displacements due to the flow of vibrational energy of the model introduced in Figure (3.1) are given below by assuming time harmonic motion at frequency ω . Therefore all quantities will vary as $e^{i\omega t}$. Thus

$$w_+(x,t) = b^+ e^{i(\omega t - kx)} + b_N^+ e^{i\omega t} e^{-kx}; \quad w_-(x,t) = a^+ e^{i(\omega t - kx)} + a^- e^{i(\omega t + kx)} + a_N^- e^{i\omega t} e^{kx}, \quad (3.1)$$

where w_+ and w_- are the displacements of the beam in the regions $x \geq 0$ and $x \leq 0$ respectively, and the amplitudes a and b may be complex. The flexural wavenumber k is given previously in Eq.(2.8)

The wavenumber is real and positive, unless damping is present where it will have a negative (and usually small) imaginary part [11].

The five wave components represent respectively positive-going (a^+) and negative-going (a^-) propagating waves, a positive-going transmitted (propagating) wave (b^+) and the two nearfield components a_N^- and b_N^+ which can be considered as negative- and positive-going evanescent waves in the regions $x \leq 0$ and $x \geq 0$ respectively.

In the reminder of this section, the reflection and transmission coefficients for a passive dynamic absorber attached to a thin beam will be derived.

3.2 Reflection & Transmission Coefficients.

If a propagating wave is incident upon some discontinuity in the beam^{*}, it will give rise to reflected (a^- , a_N^-) and transmitted (b^+ , b_N^+) waves whose amplitudes and phases are given by reflection and transmission coefficients, where

$$a^- = ra^+, \quad b^+ = ta^+, \quad a_N^- = r_N a^+, \quad \text{and} \quad b_N^+ = t_N a^+. \quad (3.2)$$

Here t and r are the transmission and reflection coefficients as described in chapter two.

The reflection and transmission coefficients of the thin beam like structure with an attached undamped absorber can be found by considering the continuity and equilibrium equations of the system.

Continuity of displacement gives $w_+(0) = w_-(0)$ and hence

$$b^+ + b_N^+ = a^+ + a^- + a_N^-. \quad (3.3)$$

Continuity of rotation ($\partial w_+(0)/\partial x = \partial w_-(0)/\partial x$) gives

$$-ib^+ - b_N^+ = -ia^+ + ia^- + a_N^-. \quad (3.4)$$

The shear forces and bending moments at cross sections of the beam at either side of the absorber are shown in Figure (3.2)

* The same model will be discussed later with an incident evanescent wave

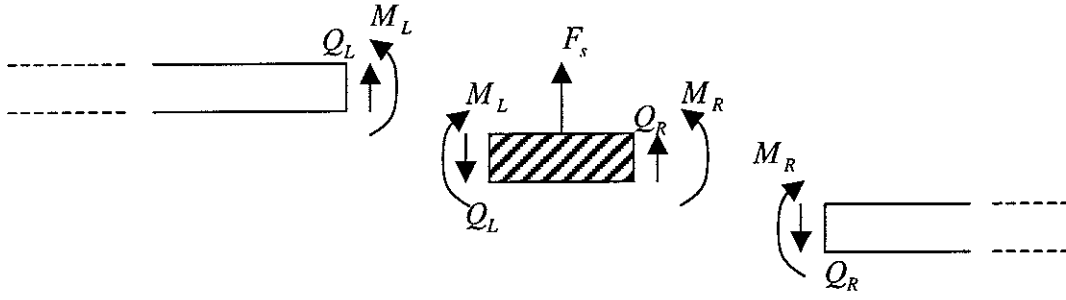


Figure 3.2 Shear forces and bending moments at either side of the absorber

Equilibrium of forces then implies $Q_R - Q_L = -F_s$, where $F_s = \bar{k}_t(y - w)$ is the force from the spring on the beam, y is the displacement of the absorber mass and w is the displacement of the beam at the absorber location. Therefore

$$ib^+ - b_N^+ - ia^+ + ia^- - a_N^- = \frac{\bar{k}_t}{EI k^3}(y - w). \quad (3.5)$$

The equilibrium of moments gives $M_R = M_L$, so that

$$-b^+ + b_N^+ = -a^+ - a^- + a_N^-. \quad (3.6)$$

Finally, the equation of motion for the absorber mass follows from the free body diagram of the mass shown in Figure (3.3) is given by

$$-F_s = m \frac{\partial^2 y}{\partial t^2} = -\bar{k}_t(y - w), \quad (3.7)$$

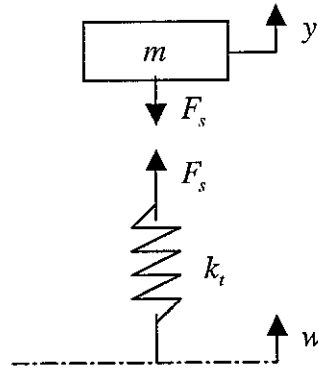


Figure (3.3) Free body diagram of the absorber mass

Therefore,

$$y = w \left(\frac{\bar{k}_t}{\bar{k}_t - m\omega^2} \right). \quad (3.8)$$

Substituting Eq.(3.8) into Eq.(3.5) gives

$$ib^+ - b_N^+ - ia^+ + ia^- - a_N^- = \frac{w}{Elk^3} \left(\frac{m\omega^2 \bar{k}_t}{\bar{k}_t - m\omega^2} \right) \quad (3.9)$$

Simplifying Eq.(3.9) gives

$$ib^+ - b_N^+ - ia^+ + ia^- - a_N^- = \frac{4\alpha}{1-\Omega^2} w, \quad (3.10)$$

where the dimensionless parameters

$$\alpha = \frac{m\omega^2}{4Elk^3} = \frac{\pi m}{2\rho A\lambda}, \quad (3.11)$$

and

$$\Omega^2 = \frac{m\omega^2}{\bar{k}_t} = \frac{\omega^2}{\omega_a^2}, \quad (3.12)$$

represent respectively, the ratio of the mass of the absorber to the mass of the beam in a length of $2\lambda/\pi$ and the frequency ratio $\Omega = \omega/\omega_a$, where $\omega_a = \sqrt{\bar{k}_t/m_a}$ is the absorber frequency.

Equations (3.2), (3.3), (3.5) and (3.9) can be solved for the reflection and transmission coefficients. These are given by

$$\begin{aligned} r &= \frac{i\alpha}{(\Omega^2 - 1) - \alpha(1+i)}; \\ t &= \frac{(\Omega^2 - 1) - \alpha}{(\Omega^2 - 1) - \alpha(1+i)}; \\ r_N = t_N &= \frac{\alpha}{(\Omega^2 - 1) - \alpha(1+i)}, \end{aligned} \quad (3.13)$$

The reflection coefficient of the propagating wave is the same as the reflection (and transmission) coefficient of the nearfield wave apart from a factor of $-i$, which is equal to a 270° phase shift.

These reflection and transmission coefficients were also formed using the dynamic stiffness method as shown in Appendix A5.0.

3.3 Tuning The Neutraliser.

The mass ratio α is frequency dependent; therefore another dimensionless parameter (γ) was derived, which is independent of the frequency ratio. This is defined in terms of the wavelength λ_a at the absorber frequency $\omega = \omega_a$. The bending wavelength therefore

$$\lambda = \lambda_a \Omega^{-1/2}, \quad (3.14)$$

as shown in Appendix A6.0. By substituting the equation above in Eq.(3.11), the mass ratio is found to be the product of two dimensionless factors as given by

$$\alpha = \gamma \Omega^{1/2}, \quad (3.15)$$

The new dimensionless parameter γ represents the mass ratio at the absorber frequency and it relates the mass of the neutraliser to the mass of the beam in a length of $2\lambda_a / \pi$. it is given by

$$\gamma = \frac{\pi m_a}{2\rho A \lambda_a}. \quad (3.16)$$

Substituting Eq.(3.15) into the expressions for the reflection and transmission coefficients found in Eq.(3.13), gives alternative expressions for the coefficients, given by

$$\begin{aligned} r &= \frac{i\gamma\Omega^{1/2}}{(\Omega^{1/2}-1) - \gamma\Omega^{1/2}(1+i)}; \\ t &= \frac{(\Omega^2-1) - \gamma\Omega^{1/2}}{(\Omega^2-1) - \gamma\Omega^{1/2}(1+i)}; \\ r_N = t_N &= \frac{\gamma\Omega^{1/2}}{(\Omega^2-1) - \gamma\Omega^{1/2}(1+i)}. \end{aligned} \quad (3.17)$$

Hence Ω depends only on frequency while γ is the mass ratio at the absorber frequency. The purpose of the neutraliser introduced here is to control the transmission of flexural waves on a beam. This has been discussed previously with some differences by Clark [4] and Brennan [5]. In the ideal performance of the undamped neutraliser, no waves manage to transmit to the downstream region. All the incident energy is reflected back in the direction of the source of injection. Damping in the neutraliser adversely affects its performance in controlling the transmission of the incident waves *.

* This will be validated later on using two models, one includes a spring element with hysteretic damping and the other model includes a damping element.

Thus in order to achieve zero transmission, one finds that the tuned frequency is such that $t = 0$ in Eq.(3.17) and this satisfies

$$\Omega^2 - \gamma\Omega^{1/2} - 1 = 0. \quad (3.18)$$

This will result in four roots for each mass ratio γ . Only one of these roots is a real positive number and is defined to be the tuning frequency ratio Ω_t at which there are no transmitted waves. This will be explained in the next chapter.

3.4 General Discussion.

The reflection and transmission analysis presented in this report depends on two unique independent parameters (Ω and γ), and these can be used in simplifying the control of the transmission of flexural waves on a beam.

Some limiting cases can be used for validating the reflection and transmission coefficients. When the mass of the absorber is very large, then Eq.(3.17) reduces to

$$\begin{aligned} r &= -\frac{(1+i)}{2}; \\ t &= \frac{(1-i)}{2}; \\ r_N &= t_N = -\frac{(1-i)}{2}, \end{aligned} \quad (3.19)$$

These are the same values as those for a pinned joint discontinuity as expected.

If either the mass or stiffness of the absorber is insignificant, then the transmission coefficient will have a value of 1, which indicates zero reflection hence there is no suppression of flexural waves occurred. Again this is expected.

The undamped absorber will behave as an attached mass if the stiffness of the spring is very large*, and this has been verified numerically. Eq.(3.17) reduce to

$$\begin{aligned} r &= \frac{\alpha}{i - \alpha(1-i)}; \\ t &= \frac{i(1+\alpha)}{i - \alpha(1-i)}; \\ r_N &= t_N = \frac{-i\alpha}{i - \alpha(1-i)}, \end{aligned} \quad (3.20)$$

Note that the dimensionless factor α used in Appendix A1.0 has a negative sign.

* The mass will behave as if it were rigidly attached to the beam.

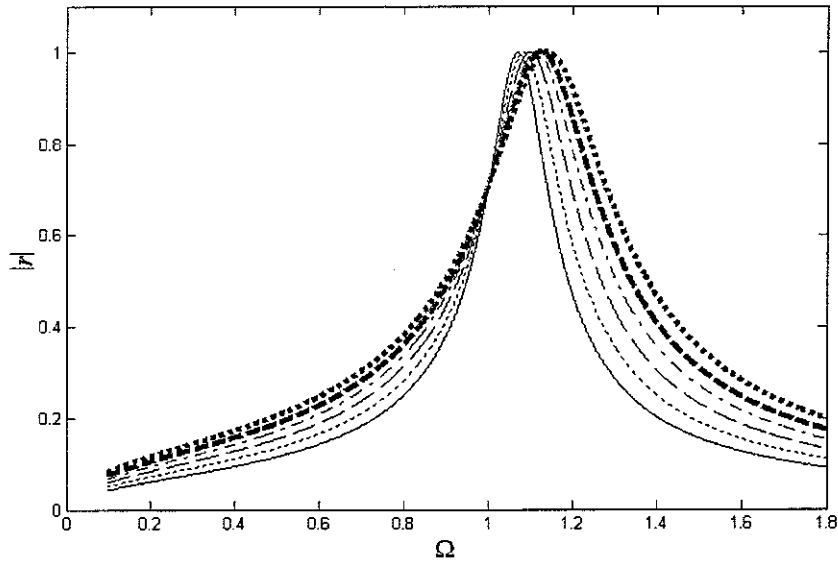
4- NUMERICAL EXAMPLES.

This chapter comprises three main sections, and these investigate the dynamic behaviour of the undamped neutraliser. The first section concerns the reflection and transmission coefficients as function of the frequency and mass ratio parameters while the second section investigates the energy behaviour around the discontinuity and conservation of energy carried by the propagating waves along the thin beam. The final section concerns the bandwidth.

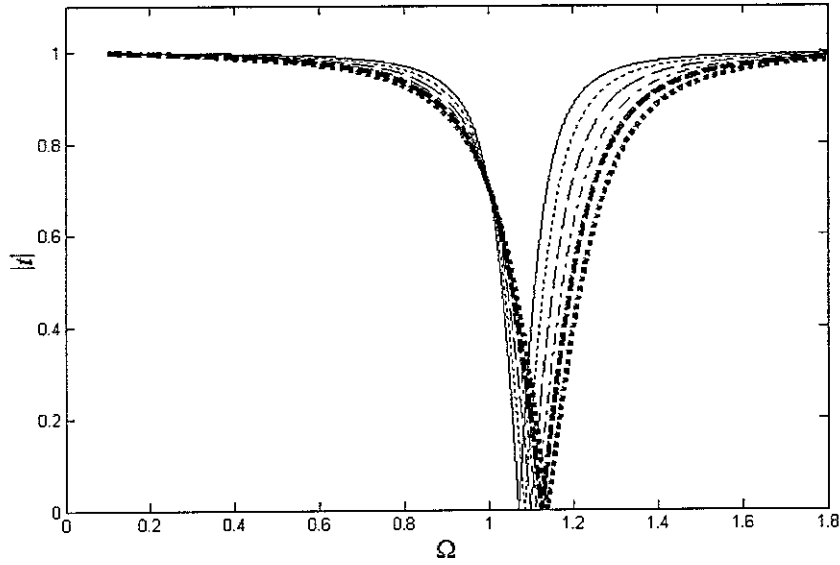
4.1 Relation Between, r , t , Ω and γ .

The aim of this section is to investigate the dynamic behaviour of the undamped absorber and beam, and to show how the flexural wave transmitted along the beam is suppressed at a specified tuning frequency.

Consider an infinite beam with an undamped neutraliser fitted as shown in Figure (3.1). The effects of neutraliser on the response of the reflection and transmission coefficients for different mass ratios are shown in Figure (4.1 a, b).



-a-



-b-

Figure 4.1. Magnitude of the reflection and transmission coefficients as function of the frequency ratio Ω . (a) Reflection $|r|$; (b) Transmission $|t|$.

— $\gamma = 0.14$; $\gamma = 0.1675$; ----- $\gamma = 0.1975$; - · - · - $\gamma = 0.2250$;
 - - - $\gamma = 0.2525$; $\gamma = 0.2825$.

For $\Omega < \Omega_t$, the reflection coefficient for all the mass ratios increases until a specific frequency ratio $\Omega = \Omega_t$ is reached where $|r| = 1$ and the entire incident propagating wave is reflected back. Moreover, for each mass ratio there is a specific tuned frequency Ω_t at which transmission of the incident propagating wave is fully suppressed.

The reflection coefficient decreases with frequency ratio greater than the tuned frequency. When the forcing frequency coincides with the natural frequency of the absorber ($\Omega = 1$), then the magnitude of the reflection coefficient has the same value of $1/\sqrt{2}$ for any given mass ratio. In the same way the transmission coefficient decreases as the mass ratio increases for frequencies less than the tuning frequency Ω_t as shown in Figure (4.1b). This again shows that the transmission coefficient decreases gradually as the frequency ratio increases until the mentioned tuning frequency Ω_t is reached at which none of the incident propagating waves is transmitted.

It was found that the neutraliser has a profound effect at one specific frequency on the transmitted flexural wave, and this effect reduces gradually as the frequency ratio moves away from the tuned frequency.

The reason that the neutraliser is ineffective at frequencies other than the tuned frequency can be explained by considering the dynamic stiffness (k_{eff}) of the neutraliser, which is given by [7]

$$k_{eff} = \frac{-m\omega^2}{1 - \Omega^2}. \quad (4.1)$$

Hence the dynamic impedance (Z) was found below.

$$Z = \frac{m\omega i}{1 - \Omega^2}.$$

This has to be infinite if the neutraliser is placed at the point of excitation, and this is satisfied if the tuned frequency ratio $\Omega_t = 1$.

Below the natural frequency (i.e. $\Omega < 1$), the dynamic stiffness of the neutraliser is mass-like. r and t of mass discontinuity was found in appendix A7.0. Figure 7.1 shows that the neutraliser is ineffective at low frequencies. On the other hand, the neutraliser behaves as a spring discontinuity at frequencies greater than the neutraliser's natural frequency (i.e. $\Omega > 1$). At one specific tuned frequency, the incident propagating wave is fully reflected and nothing is transmitted and this effect reduces at higher frequencies as shown in Figure A4.0.

4.2 Conservation of Energy.

The reflection and transmission of power due to wave motion* in a beam like structure with an undamped absorber have been investigated. Assuming no dissipation of energy takes place, then the power through a discontinuity behaves in a way such that.

$$|t|^2 + |r|^2 = 1. \quad (4.2)$$

This is the conservation of energy, where the energies in the reflection and transmission waves equal that of the incident wave.

Thus if there is no discontinuity to suppress the flexural waves, then the reflection coefficient in the equation above is zero and all the power is transmitted.

* Energy is directly proportional to the square of wave amplitude.

This equation is satisfied both analytically and numerically by adding the square of each magnitude value of the reflection and transmission coefficients in Eq.(3.13). The powers in the reflected and transmitted waves are shown in Figures (4.2 a, b).

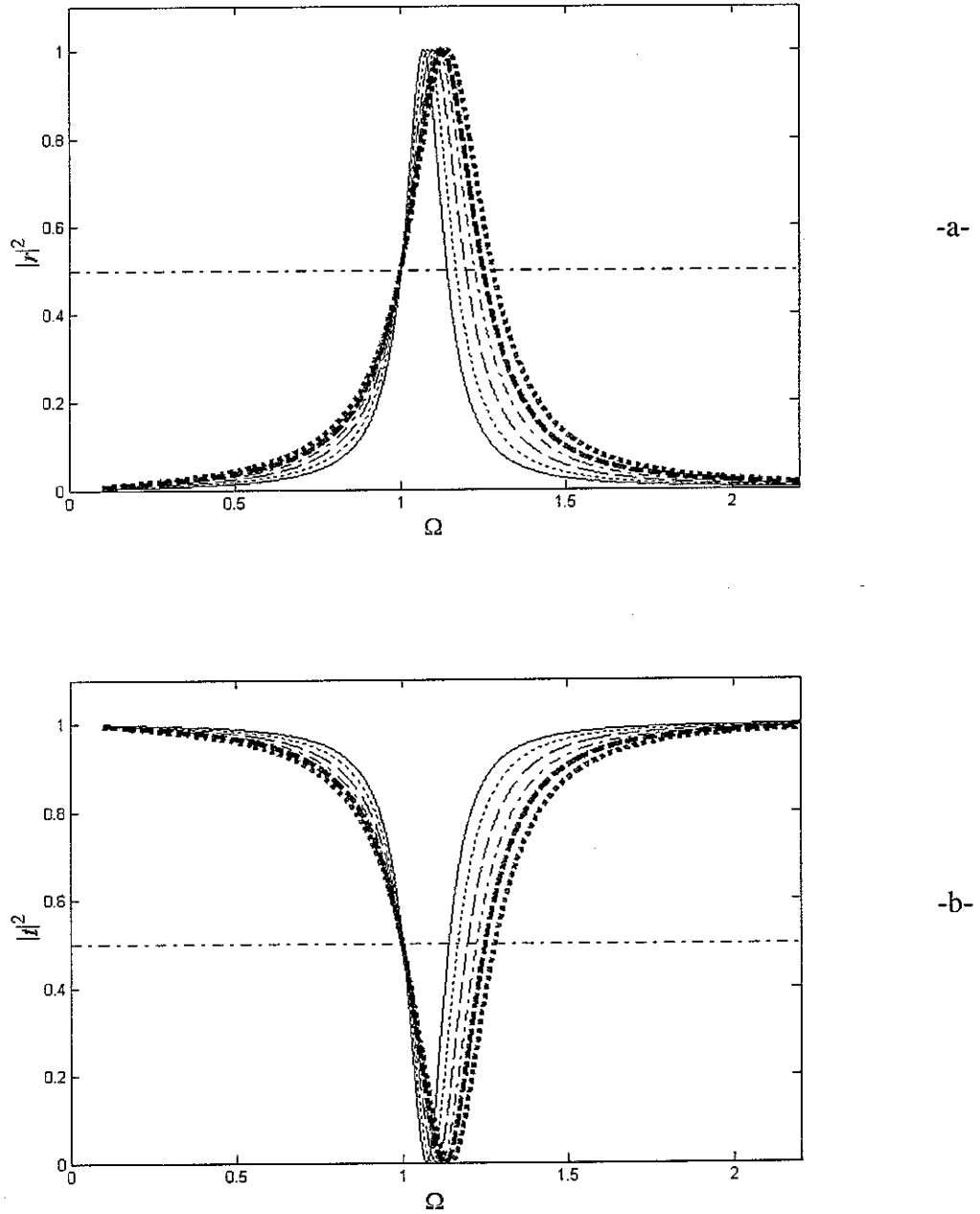


Figure 4.2. Powers reflected and transmitted versus the frequency ratio Ω . (a) Reflected wave (b) Transmitted wave.

— $\gamma = 0.14$; — $\gamma = 0.1675$; - - - $\gamma = 0.1975$; - · - · $\gamma = 0.2250$;
 - - - $\gamma = 0.2525$; · · · $\gamma = 0.2825$.

Increasing the mass ratio γ has a major effect on the range of frequencies over which less than half the incident power is transmitted. This will be discussed later.

Half the power is reflected when the neutraliser's natural frequency coincides with the forcing frequency (i.e. $\Omega = 1$) and all of the power is reflected back at the tuned frequency for any given mass ratio.

The conservation of energy is validated and plotted in Figure (4.3). Thus it proves that there is no dissipation of energy as expected.

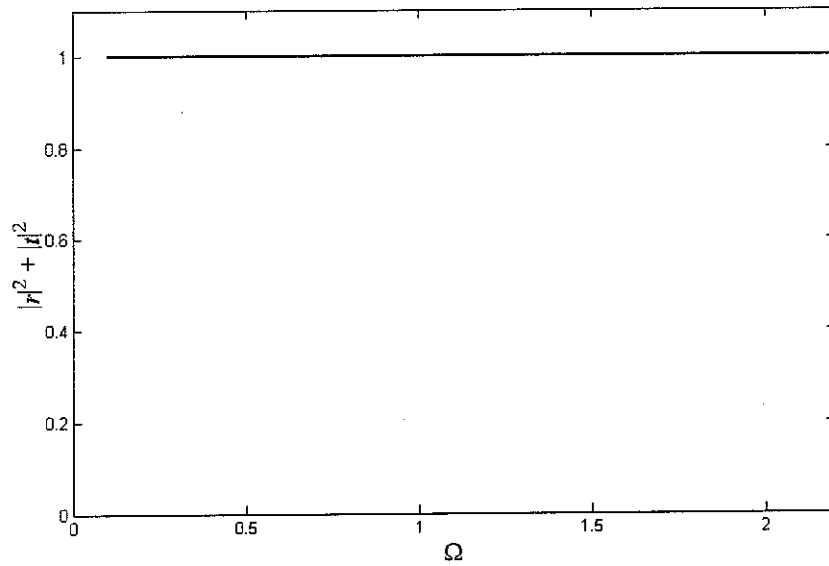


Figure 4.3. Conservation of Energy for any given mass ratio

4.3 The Width Variation of the Transmission Stop-Band.

It was seen above that as the frequency ratio Ω increases, the transmitted power $|t|^2$ decreases from unity and it is 0.5 at $\Omega = 1$, zero at $\Omega = \Omega_r$, and increases to unity again as $\Omega \rightarrow \infty$.

The bandwidth $\Delta\Omega$ here is defined as the range of frequencies in which less than half the incident power is transmitted, i.e. where $|t|^2 \leq 1/2$, it is bounded by two half-power points where $|t|^2 = 1/2$. The lower half-power point Ω_1 for all given mass ratios has the value of 1 as shown in Figure (4.2b).

The upper half-power point Ω_2 depends on the mass ratio γ . Increasing the mass of the neutraliser increases the bandwidth $\Delta\Omega$.

Taking the square of the modulus of Eq.(3.17b) and setting this equal to 0.5, one can find the upper half-power point by solving the equation below

$$\Omega^2 - 2\gamma\Omega^{1/2} - 1 = 0, \quad (4.3)$$

for Ω . Only one of the roots is a real positive number and represents the upper half-power point Ω_2 , which depends on γ .

One can find the tuning frequency Ω_t for each value of γ , by solving Eq.(3.18) as mentioned in the previous section. Zero transmission is satisfied at that frequency.

Increasing the mass ratio γ will cause the zero transmission at higher tuning frequencies as shown in Figure (4.4), which introduce a comparison between Ω_2 , Ω_t , and $\Delta\Omega$ versus the mass ratio γ .

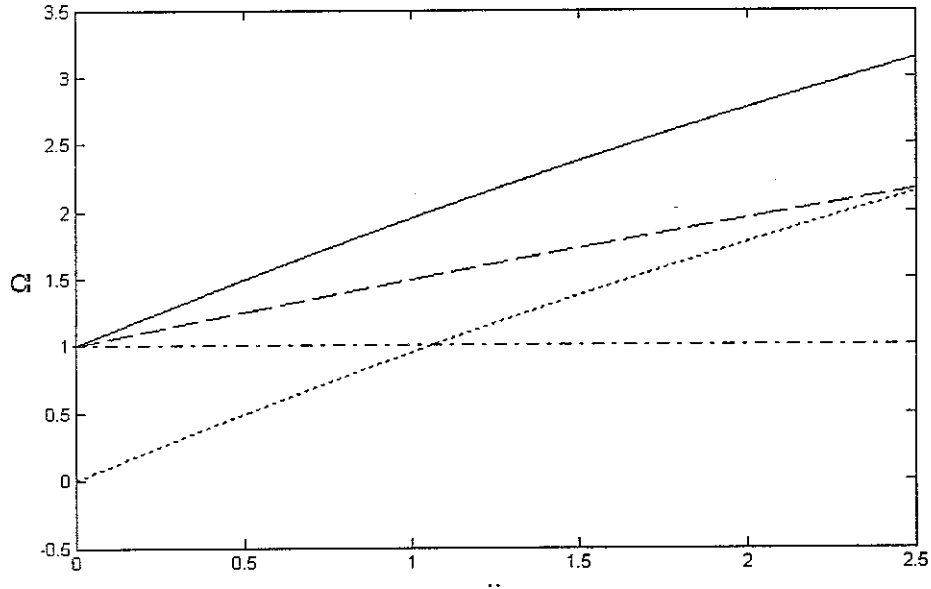


Figure 4.4. The effect of varying the mass ratio γ on Ω_2 , Ω_t , and $\Delta\Omega$.

— Ω_2 ; - - - Ω_t ; $\Delta\Omega$; - . - . Ω_1

Increasing the mass ratio γ has increased the effectiveness of the neutraliser by increasing the bandwidth $\Delta\Omega$ as a result of increasing the frequency ratio of the upper-power point Ω_2 . The relation between the bandwidth and the upper half-power point is given by

$$\Delta\Omega = \Omega_2 - 1. \quad (4.4)$$

Therefore, increasing the mass ratio will increase the upper half power point and this the bandwidth of attenuation,

One can find from Eq.(3.18) and Eq.(4.3), that the tuned frequency Ω_t and the upper half-power point Ω_2 of the bandwidth approaches to 1 at a very low mass ratio γ . Zero bandwidth $\Delta\Omega$ is obtained at mass ratio $\gamma=0$, where the upper half-power point Ω_2 has the same value as the lower half-power point $\Omega_1 = 1$.

However, the tuned frequency Ω_t at which no power is transmitted is approximately located in the middle of the bandwidth $\Delta\Omega$ as shown in Figure (4.2b).

5- CONCLUSIONS & DISCUSSION.

This chapter highlights some general remarks of the previous chapters and the scheduled future work.

5.1 General Concluding Remarks.

Analytical and numerical investigations have been carried out into the use of undamped tunable neutraliser to suppress incident propagating waves in thin beams. The effect of propagating waves as they transmit energy through beam structure has been shown briefly. In addition, evanescent waves may cause energy to flow via the interaction of any two opposite decaying nearfields. The feature becomes of practical significance in structures with discontinuities or constraints on which evanescent waves of various directions are generated.

Numerical wave model of the undamped vibration neutraliser was found for optimal isolation. Reflection and transmission of flexural waves were determined including nearfield waves with respect to the incident propagating one. These have included new independent parameters for design and control simplicity purposes.

The optimum characteristics of the neutraliser, which ensures zero transmission, have been determined. The conservation of energy flowing through the beam has been satisfied numerically. Although the bandwidth introduced by other workers are very effective in measuring the performance of the damped neutraliser but it was necessary to employ another definition for the ideal undamped neutraliser.

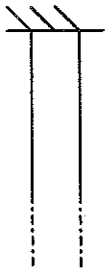

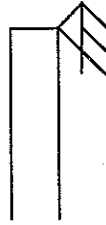
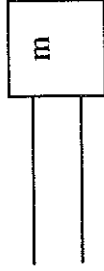
5.2 Future Work.

- Numerical wave model of the vibration neutraliser for optimal absorption will be developed in the presence of nearfields.
- Experimental work will be carried out to investigate the validity of the numerical and analytical model of the optimum absorption neutraliser.
- A control system will be implemented by adopting the gradient descent algorithm for fine-tuning such as those described by Kuo and Morgan [16].
- The estimated flexural wave amplitudes will be used as a cost function in the control system.

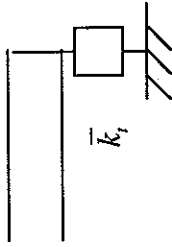
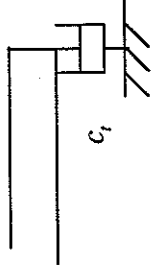
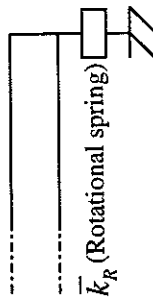

APPENDICES

A1.0 Reflection & Transmission Coefficients of Flexural Waves due to Boundary/Discontinuity in beam structures.

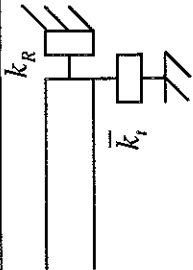
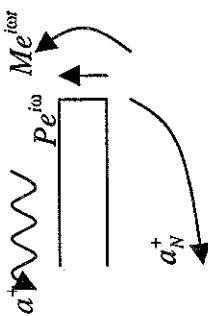
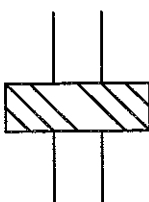
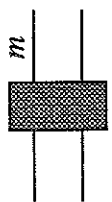
This appendix presents the result of a wide survey on reflection and transmission of flexural waves in beam structures due to various discontinuities and boundary conditions. Reflection and transmission of waves were tabulated below (Table A1.0) of well-known models of beam structures for incident propagating nearfield (the effect of a single decaying nearfield has been investigated for a translational spring discontinuity). These were determined at $x=0$ by considering continuity and equilibrium conditions.

Type	Diagram	r	t	r_N	t_N	Dimensionless factor
Clamped End		$-i$	-	$-(1-i)$	-	-
Free End		$-i$	-	$(1-i)$	-	-
Pinned Boundary		$r = -1$	-	$r_N = 0$	-	-
Mass attached at free End		$r = -\frac{1+i+2\mu}{1-i+2\mu}$	-	$r_N = -\frac{2i}{1-i+2\mu}$	-	$\mu = \frac{m\omega^2}{Ek^3}$

Continued:

Type	Diagram	r	t	r_N	t_N	Dimensionless factor
Spring attached at free end		$r = -\frac{1+i-2\varepsilon}{1-i-2\varepsilon}$	-	$r_N = -\frac{2i}{1-i-2\varepsilon}$	-	$\varepsilon = \frac{\bar{k}_T}{Elk^3}$
Damped attached at free end		$r = -\frac{1+i-2i\alpha}{1-i-2i\alpha}$	-	$r_N = -\frac{2i}{1-i-2i\alpha}$	-	$\alpha = \frac{\omega c_t}{Elk^3}$
Rotational spring at free end		$r = -\frac{1+i+2ik_R}{1-i-2ik_R}$	-	$r_N = -\frac{2i}{1-i-2ik_R}$	-	$k_R = \frac{\bar{k}_R}{Elk}$
Slider attached to the free end		$r = 1$	-	$r_N = 0$	-	-

Continued:

Type	Diagram	r	t	r_N	t_N	Dimensionless factor
Rotational and translational springs at free end		$r = -\frac{1+i+2ik_R-2k_t-k_tk_R-ik_tk_R}{1-i-2ik_R-2k_t-k_tk_R+ik_tk_R}$	-	$r_N = \frac{k_t+i}{k_t-1} \left(\frac{i-k_t}{k_t-1} + r \right)$	-	$\frac{k_R = \bar{k}_R / EIk}{k_t = \bar{k}_t / EIk^3}$
Bending moment & Harmonic force applied at free end		$a^+ = -\frac{(1+i)}{2} \frac{Mk}{EIk^3}$ $a_N^+ = -\frac{(i-1)(Mk-P)}{2} \frac{P}{EIk^3} + \frac{P}{EIk^3}$	-	-	-	-
Slider Discontinuity		$r = \frac{1-i}{2}$	$t = \frac{1+i}{2}$	$r_N = \frac{i-1}{2}$	$t_N = \frac{1-i}{2}$	-
Mass Discontinuity		$r = \frac{i\alpha}{4-\alpha(1+i)}$	$t = \frac{4-\alpha}{4-\alpha(1+i)}$	$r_N = \frac{\alpha}{4-\alpha(1+i)}$	$t_N = r_N$	$\alpha = -\frac{m\omega^2}{EIk^3}$

Continued:

Type	Diagram	r	t	r_N	t_N	Dimensionless factor
Spring Discontinuity		$r = \frac{i\varepsilon}{4 - \varepsilon(1+i)}$	$t = \frac{4 - \varepsilon}{4 - (1+i)}$	$r_N = \frac{\varepsilon}{4 - \varepsilon(1+i)}$	$t_N = r_N$	$\varepsilon = \frac{\bar{k}_t}{Elk^3}$
Damper Discontinuity		$r = \frac{i\mu}{4 - \mu(1+i)}$	$t = \frac{4 - \mu}{4 - \mu(1+i)}$	$r_N = \frac{\mu}{4 - \mu(1+i)}$	$r_N = t_N$	$\mu = \frac{i\omega c_t}{Elk^3}$
Discontinuity of rotational spring		$r = \frac{-ik_R}{4 + k_R(1-i)}$	$t = \frac{4 + k_R}{4 + k_R(1-i)}$	$r_N = r$	$t_N = -r$	$k_R = \frac{\bar{k}_R}{Elk}$
Discontinuity of harmonic force		$a^+ = \frac{iF}{4Elk^3} = a^-$ $a_N^+ = \frac{F}{4Elk^3} = a_N^-$	-	-	-	-

Continued:

Type	Diagram	r	t	r_N	t_N	Dimensionless factor
Harmonic moment discontinuity		$a^+ = \frac{M}{4EK^2} = a_N^-$ $a^- = -\frac{M}{4EK^2} = a_N^+$	-	-	-	-
Spring Discontinuity (Incident Nearfield)		$r = \frac{a^-}{a_N^+} = \frac{K_i}{4i + K_i(1-i)} = \frac{b^+}{a_N^+} = t$ $t_N = \frac{b_N^+}{a_N^+} = \frac{4i + K_i}{4i + K_i(1-i)}$ $r_N = \frac{a_N^-}{a_N^+} = \frac{iK_i}{4i + K_i(1-i)}$	-	-	-	$K_i = \frac{\bar{k}_i}{EK^3}$

Table A1.0

Where the flexural waves mentioned in Table A1.0 have the following terms.

a^+ = Positive propagating wave.

a^- = Negative propagating wave.

- a_N^+ = Positive evanescent wave.
- a_N^- = Negative evanescent wave.
- b^+ = Positive transmitting wave.
- b^- = Negative transmitting wave.
- b_N^+ = Positive transmitting wave.
- b_N^- = Negative transmitting wave.

These were illustrated in Figure A1.0 below.

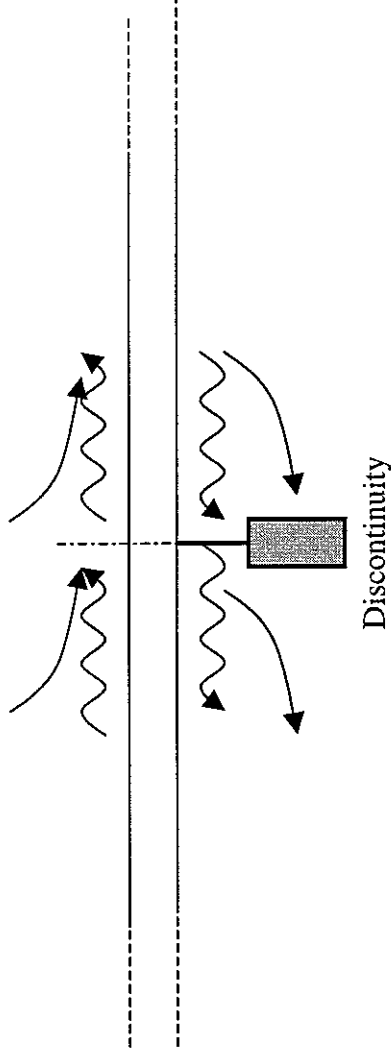
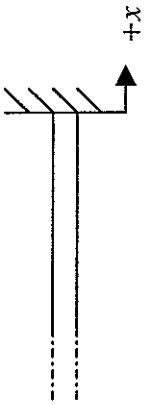
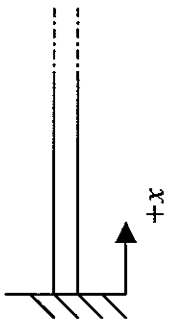

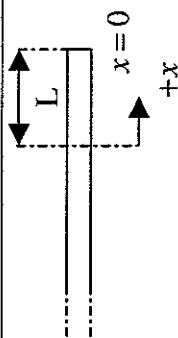
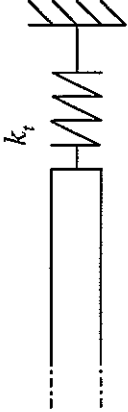


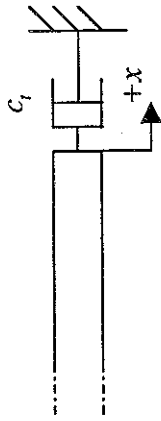
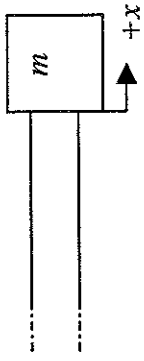
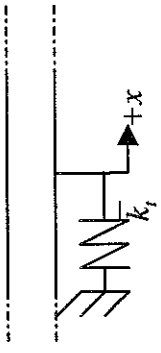
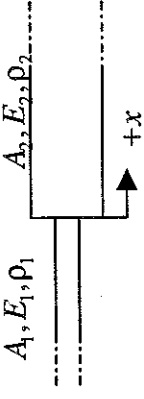
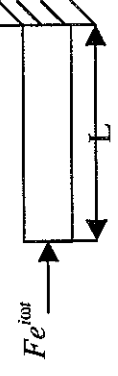
Figure A1.0. Flexural waves around the point discontinuity.

A2.0 Reflection & Transmission Coefficients of Longitudinal Waves due to Boundaries/Discontinuities in bar structures.

The reflection and transmission coefficients of longitudinal waves in bar structures have been investigated for various boundaries/discontinuities. These were determined at $x=0$ by considering continuity and equilibrium conditions and tabulated below (Table A2.0).

Type	Diagram	r	t	Dimensionless factor
Clamped at right end		$r = -1$	-	-
Clamped at left end		$r = -1$	-	-
Free end		$r = 1$	-	-
At distance L from free end		$r = e^{-2iL}$	-	-
Spring at free end		$r = -\frac{1 - \varepsilon i}{1 + \varepsilon i}$	-	$\varepsilon = \frac{E A k}{\bar{k}_t}$

Continued:

Type	Diagram	r	t	Dimensionless factor
Damper at free end		$r = -\frac{1-i\mu}{1+i\mu}$	-	$\mu = \frac{E A k}{c_t \omega}$
Mass at free end		$r = -\frac{1+i\alpha}{1-i\alpha}$	-	$\alpha = \frac{E A k}{m \omega^2}$
Spring Discontinuity		$r = -\frac{1}{1+2i\varepsilon}$	$t = 1-r$	$\varepsilon = \frac{E A k}{k_t}$
Change in Cross section		$r = \frac{A_1 - A_2}{A_1 + A_2}$	$t = \frac{2A_1}{A_1 + A_2}$	-
Harmonic force at free end		$r = -e^{-2i\omega L}$	-	-

Continued:

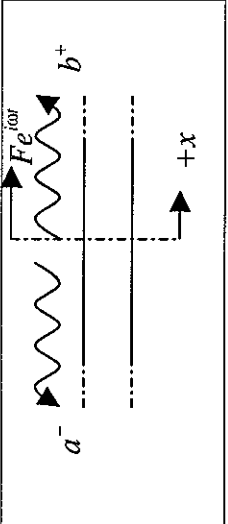
Harmonic Force as a discontinuity		$b^+ = \frac{F}{2EAki} = a^-$	-	-
-----------------------------------	---	-------------------------------	---	---

Table A2.0

A3.0 Energy Flow in the Longitudinal Travelling Waves in bar structures.

This appendix introduces the power flowing in bar structures due to propagating longitudinal waves (no nearfields in bar structures). Same methods used for the flexural waves shown in chapter 2 are used here again.

Considering both positive and negative propagating waves exist in a bar element δx , the following have been determined.

- a- Instantaneous intensity $I(x, t) = EA\omega k_l (a^{+2} \sin^2(\omega t - kx) - a^{-2} \sin^2(\omega t + kx))$.
using Eq.(2.16), where k_l is the longitudinal wavenumber.

- b- Time average intensity $\langle i(t) \rangle = \frac{EA\omega k_l}{2} (a^{+2} - a^{-2})$.

- c- The kinetic energy per unit length was found to include three terms as shown below:

$$E_{kin} = \frac{1}{2} \rho A \omega^2 (a^{+2} \sin^2(\omega t - k_l x) + 2a^+ a^- \sin(\omega t - k_l x) \sin(\omega t + k_l x) + a^{-2} \sin^2(\omega t + k_l x)).$$

- d- The potential energy per unit length was found to have same terms as the kinetic energy except that the cross power term has a negative sign as shown below.

$$E_{pot} = \frac{1}{2} \rho A \omega^2 (a^{+2} \sin^2(\omega t - k_l x) - 2a^+ a^- \sin(\omega t - k_l x) \sin(\omega t + k_l x) + a^{-2} \sin^2(\omega t + k_l x)).$$

- e- Thus the total energy per unit length was determined below and found to include only two terms (no cross power).

$$E_{tot} = a^{+2} \sin^2(\omega t - kx) + a^{-2} \sin^2(\omega t + kx).$$

- f- The phase velocity (c_B) was found to have same value as the group velocity (c_g).

$$c_g = c_B = \frac{\omega}{k}.$$

- g- The characteristic wave impedance wave (Z) determined for the longitudinal

propagating wave.
$$Z = \frac{EA |\partial u / \partial x|}{|\partial u / \partial t|} = \rho c_B A.$$

A4.0 Effect of Undamped Spring Discontinuity on Flexural Waves.

The effect of undamped springs on flexural waves in beam structures has been investigated numerically and analytically. Complete suppression of flexural waves can be achieved on infinite beam at single frequency. Reflection and transmission of flexural waves were determined below by considering the continuity and equilibrium conditions.

$$r = \frac{i\varepsilon}{4 - \varepsilon(1+i)}$$

$$t = \frac{4 - \varepsilon}{4 - \varepsilon(1+i)};$$

$$r_N = t_N = \frac{\varepsilon}{4 - \varepsilon(1+i)}$$

where

$$\varepsilon = \frac{\bar{k}}{EI k_l^3},$$

thus E , I , k and k_l have their usual meanings.

Figure A4.0 below shows clearly the effect of the undamped spring on the flexural wave

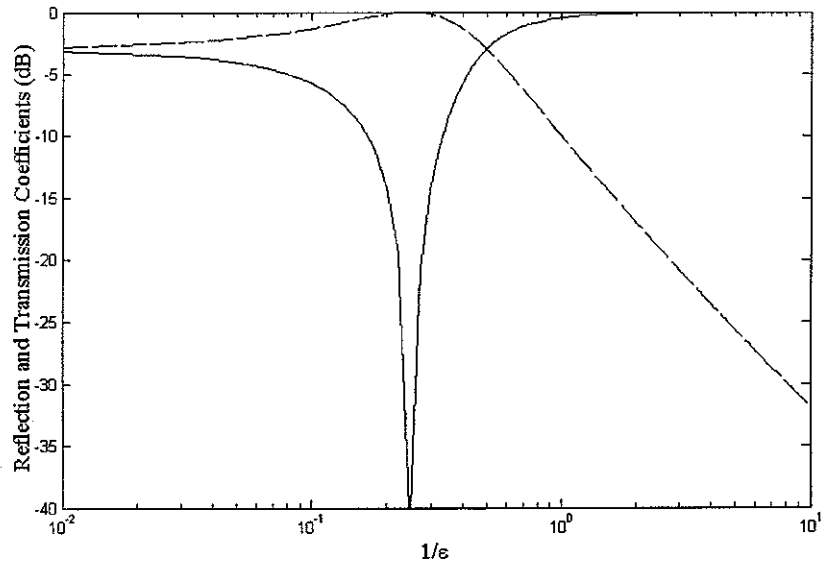


Figure A4.0. Effect of Spring Discontinuity on the flexural waves in beam structures.

(a) ———— $|t|$; - - - - - $|r|$.

Note that it is rarely possible to fix a spring to rigid foundation in practice, and thus it has to react against an inertial mass.

A5.0 Using Dynamic Stiffness Method in Finding r , t , of an undamped absorber.

The following equations can be deduced from the free body diagram shown in Figure A5.0.

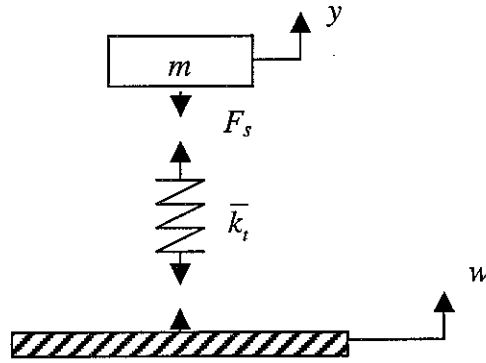


Figure A5.0. Free body diagram of the undamped absorber.

Hence one can determine the displacement (y) neutraliser's mass.

$$y = \frac{\bar{k}_t w}{\bar{k}_t - m\omega^2}. \quad (\text{A5.1})$$

That \bar{k}_t is the translational stiffness.

Substituting Eq.(A5.1) in force balance of the free body diagram above, then one can find

$$k_{eff} = -\frac{m\omega^2 \bar{k}_t}{\bar{k}_t - m\omega^2}.$$

That $k_{eff} = F / w$ is the effective dynamic stiffness of the neutraliser.

Dividing both sides by EIk^3 to obtain the dimensionless factor α . Then the dimensionless factor of the spring ϵ (given in table A1.0) was replaced by the result. Therefore, one can find that the reflection and transmission coefficients found to match those of the neutraliser determined in Chapter 2.

A6.0 Relation Between λ and Ω .

It is well known that the wavelength λ is inversely proportional to square root of the circular frequency. Therefore, from Eq.(3.13), one can find the following

$$\frac{\lambda}{\lambda_{abs}} = \frac{\sqrt{\omega_{abs}}}{\sqrt{\omega}} = \Omega^{-\frac{1}{2}},$$

where constants of proportionality cancel out. Hence,

$$\lambda = \lambda_a \Omega^{-1/2},$$

A7.0 Effect of Mass Discontinuity on Flexural Waves.

From the continuity and equilibrium equations explained in chapter three, one can find the reflection and transmission coefficients by considering an inertial mass as a discontinuity instead of an undamped neutraliser. This is also explained by Mead [6].

$$r = \frac{-i\alpha}{4 + \alpha(1+i)}$$

$$t = \frac{4 + \alpha}{4 + \alpha(1+i)};$$

$$r_N = \frac{-\alpha}{4 + \alpha(1+i)} = t_N$$

where the dimensionless factor $\alpha = 2\pi m / \rho A \lambda$ relates the neutraliser's mass to the mass of one wavelength of the beam. Figure A7.0 shows that the maximum reduction of an incident flexural wave using a mass discontinuity is only 3dB.

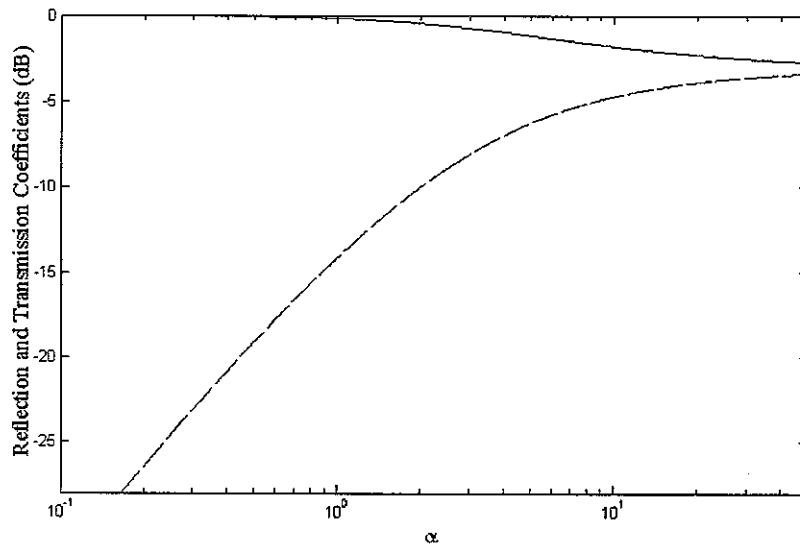


Figure A7.0. Effect of mass discontinuity of flexural waves.

— $|r|$; - - - $|t|$

REFERENCES

- 1- A. H. VON FLOTOW, A BEARD and D. BAILEY 1994 *Proceedings of Noise Con 94*, 437-454. Adaptive tuned vibration absorbers: tuning laws, tracking agility, sizing and physical implementation.
- 2- J. Q. SUN and M. R. JOLLY 1995 *Transaction of the American Society of Mechanical Engineers* (Journal of Mechanical Design), 234-242. Passive, adaptive and active tuned vibration absorbers.
- 3- M. J. BRENNAN 1997 *Proceedings of the Institution of Mechanical Engineers*, Journal of Mechanical Engineering Science **211**, 91-108. Vibration control using a tunable vibration neutraliser.
- 4- P. CLARK 1995. PhD Thesis, *University of Southampton*. Devices for the reduction of pipeline vibration.
- 5- M. J. BRENNAN 1998 *Journal of Sound and Vibration* **222(3)**, 389-407. Control of flexural waves on a beam using a tunable vibration neutraliser.
- 6- L. CREMER, M. HECKL and E. E. UNGAR 1975 *Structure – borne sound*. New York: Springer – Verlag.
- 7- J. P. DEN HARTOG 1956 *Mechanical Vibration*. McGraw – Hill Book Company.
- 8- R. E. D. BISHOP, D. C. JOHNSON 1960 *Mechanics of Vibration*. Cambridge university press.
- 9- S. TIMOSHENKO, D. H. YOUNG and W. WEAMER 1974 *Vibration Problems in Engineering* 4th Edition. John Wiley & Sons Inc.
- 10- K. F. GRAFF 1975 *Wave motion in elastic solids*. Dover Publications, Inc., New York.
- 11- B. R. MACE 1984 *Journal of Sound and Vibration* **97(2)**, 237-246. Wave reflection and transmission in beams.
- 12- B. R. MACE and C. R. HALKYARD 1995 *Journal of sound and Vibration* **230(3)**, 561-589. Time domain estimation of response and intensity in beams using wave decomposition and reconstruction.

- 13- H. G. D. GOYDER and R. G. WHITE 1979 *Journal of Sound and Vibration* **68(1)**, 59-75. Vibrational power flow from machines into built-up structures, Part 1: Introduction and approximate analyses of beam and plate – like foundations.
- 14- YU. I. BOBROVNITSKII 1992 *Journal of Sound and Vibration* **152**, 175-176. On the energy flow in evanescent waves.
- 15- W. GOUGH, J. P. G. RICHARDS and R. P. WILLIAMS 1983 *Vibration and waves*. John Wiley & Sons, Inc
- 16- S. M. KUO and D. R. MORGAN 1996 *Active Noise Control Systems, Algorithms and DSP Implementations* New York: John Wiley and Sons, Inc .
- 17- D. J. MEAD 1982 In *Noise and Vibration* (R. G. WHITE and J. G. WALKER, editors) Chapter 9. Ellis Horwood Publishers, Chichester. Structural wave motion.

